

Numerical Model of a Reinforced Concrete Building: Earthquake Analysis and Experimental Validation

Roberto Nascimbene

Received 15-05-2015, accepted 18-09-2015

Abstract

Shaking-table experiments of relatively large-scale specimens play a fundamental role in deepening our understanding of seismic response of existing structures and verification of numerical models. However, and in apparent contradiction, the preparation of such a dynamic laboratory experiment requires a-priori advanced numerical simulations, necessary to both fine-tune the test specimen properties and calibrate the input motion, as a function of the objectives of the test and capabilities and characteristics of the shaking table. This research thus concerns the development of a fibre-based finite elements model of a half-scale 3D reinforced concrete frame tested under dynamic conditions at the European Centre for Training and Research in Earthquake Engineering (EUCENTRE, Pavia, Italy). Since this reduced-scale specimen is very much based on a full-scale counterpart previously tested under pseudo-dynamic conditions at the European Laboratory for Structural Assessment (ELSA) of the Joint Research Centre (JRC, Ispra, Italy), the first part of the work consisted in verifying that the software tool employed in the numerical simulations was capable of duplicating the pseudo-dynamic real test results. Having successfully met the latter objective, the second part of the work consisted in the attempted numerical simulation of the shaking table tests, with a view to ascertain that the response of the model will be within the envisaged response targets and that the necessary input motion is compatible with the shaking-table characteristics.

Keywords

Numerical simulation · fibre-based analysis · nonlinear analysis · time history analysis · pushover · rc structures

Roberto Nascimbene

European Centre for Training and Research in Earthquake Engineering, Via Ferrata 1, 27100, Pavia, Italy
e-mail: roberto.nascimbene@eucentre.it

1 Introduction

Recent major earthquakes in the Italian territory have reaffirmed the seismic vulnerability of reinforced concrete (RC) buildings typical of the past Italian building practice, highlighting structural deficiencies observed during previous events and mostly related to the transfer of the horizontal forces between structural, non-structural elements and horizontal diaphragm (Belleri et al. [1]). On site investigations explained the major structural deficiencies of RC structures and facilities, emerged from the 1998 Adana-Ceyhan (Adalier and Aydingun [2]) and 1999 Kocaeli and Duzce earthquakes (Saatcioglu et al. [3]; Sezen and Whittaker [4]), by means of inadequate stiffness and strength and/or problems caused by insufficient connections detailing. More recently, in the Italian context, the 2009 L'Aquila earthquake highlighted many criticalities, confirming the need of considering infill panel-to-structure connection failures as a further limit state to be controlled in conventional design procedures (Toniolo and Colombo [5]; Brunesi et al. [6]; Augenti and Parisi [7]). Similar deficiencies were observed by Ghosh and Cleland [8] during the 2010 Chilean earthquake. The Emilia earthquakes (Lauciani et al. [9]; Belleri et al. [1, 10]), May 20th and 29th 2012, reaffirmed the seismic vulnerability of RC buildings typical of the past Italian building practice (Bellotti et al. [11]).

As a consequence, in the European seismic countries the assessment of existing structures is a priority (Mpampatsikos et al. [12]), since the vast majority of the residential buildings was designed according to out-of-date seismic codes (or even to non seismic codes). In most of these structures, the uncertainties about the nonlinear behaviour are relevant: generally, the presence and location of potential inelastic zones, as well as their ductility capacity, are not known. As a consequence of major earthquakes, the continuous occurrence of heavy damages, underline the need of reliable methodologies for analysis, modelling, and assessment of existing constructions, taking into account the complex interaction between structural and non-structural elements to obtain more accurate informations on the non linear dynamic response of the buildings (Caprili [13]). Two different approaches may be used in the seismic verification

of infilled three dimensional RC frames: empirical methods and mechanical methods as clearly defined by Calvi et al. in [14]. Empirical methods are mostly valid for a qualitative vulnerability analysis in terms of damage probability matrices - DPM (Whitmann et al. [15]), numerical vulnerability indexes (Faccioli et al. [16]) or fragility curves (Sabetta et al. [17]; Casotto et al. [18]) which are continuous functions expressing the probability of exceeding a given damage state, given a function of the earthquake intensity. Mechanical methods, instead, provide more accurate and quantitative definition of the seismic vulnerability and are very useful for the vulnerability analysis in large areas (Singhal and Kiremidjian [19]). They provide vulnerability assessment algorithms with direct physical meaning, that not only allow detailed sensitivity studies to be undertaken, but also cater to straightforward calibration to various characteristics of building stock and hazard. On the other hand, to the purpose of obtaining more specific information about the effective seismic response of an existing RC structure, more detailed numerical approaches should be used (Cosenza et al. [20]) based on detailed structural and geometrical surveys and subsequently on the execution of nonlinear dynamic analysis (time history analysis) (Masi [21]; Sousa et al. [22]).

Basing on these observations and following the advanced numerical model procedure, with the objective of deepening the understanding of the seismic response of typical existing RC structures in the European context, a shaking-table experiment on a half-scale three dimensional irregular frame has been carried out at European Centre for Training and Research in Earthquake Engineering (EUCENTRE, Pavia, Italy). This reduced-scale specimen is based on a full-scale prototype previously tested under pseudo-dynamic conditions at the European Laboratory for Structural Assessment (ELSA) of the Joint Research Centre (JRC, Ispra, Italy), for which reason the first part of the work consists in verifying that the software that will be employed in the calibration and fine-tuning of the shaking-table experiment is able to reproduce the response of the already full-scale tested prototype. Once the latter is achieved, the second part of the work then considers the numerical simulation of the shaking table tests on the scaled specimen, with a view to ascertain that the response of the scaled model will be within the envisaged targets and that the necessary input is compatible with the shaking-table characteristics.

2 Analyzed prototype building

The full-scale prototype structure, as mentioned above, is a full-scale three-storeys building constructed and tested at the ELSA Laboratory under the framework of the European research project SPEAR (“Seismic PErformance Assessment and Rehabilitation of existing buildings”). The specimen was “designed” and constructed following the gravity loads-only design and construction practice typical of the Southern European countries in the early 70’s Fardis [23]: use of smooth reinforcing bars, existence of slender columns with large spaced stirrups,

inclined shear reinforcement in beams, column lap splices in potential plastic hinges area, lack of detailed shear reinforcement in beam-column connections, inadequate anchorage of stirrups and irregular plan layout with a evident torsional behaviour (Coelho et al [24]). These buildings are very common because they were constructed during the European “economic boom” period, and it is thus not feasible, both from a social and an economic point of view, to replace them all with new construction. Still, however, acceptable seismic risk levels to the society must be reached, for which reason these existing structures must be assessed and retrofitted. The structural configuration of the prototype building is typical of non-earthquake resistant construction of the early 70’s, in Southern Europe and other parts of the world with similar construction practices. A side view of the building and the plan of a typical repetitive floor are presented in Figs. 1(a) and (b), respectively.

The storey height is equal to 3 m and the structure is regular in elevation. The plan configuration is non symmetric in two directions (Fig. 1(b)) with 2-bay frames spanning from 3 to 6 metres. There is the presence of a balcony on the right side; furthermore the presence of a part of the structure 1 m along x-direction (weak direction) and 0.5 m along x-direction (strong direction) longer than the rest increases the plan irregularity. This means the shifting of the centre of stiffness away from the centre of mass. Details on structural beam member dimensions and corresponding reinforcing bars were taken from Fardis and Negro [25]: eight out of nine columns have a square 25 by 25 cm cross section; the ninth column (number 2 in Fig. 1(b)) has a cross section of 25 by 75 cm. Exemplificative drawings of beams 2 and 5 (see Fig. 1b) are given in Fig. 2, whilst cross-section details of typical beams and columns can be found in Fig. 3 (refer to Fig. 1b for guidance on beam and column numbering).

The concrete compression strength was considered as equal to 26.4 N/mm^2 (Jeong and Elnashai [26]). The steel mechanical properties, on the other hand, depend on the re-bars’ diameter:

- for φ 8 mm bars: yield strength $f_y = 467 \text{ N/mm}^2$, ultimate strength $f_u = 583.67 \text{ N/mm}^2$, elastic modulus $E_1 = 206000 \text{ N/mm}^2$ and post-yield hardening ratio $E_2 / E_1 = 0.0044$
- for φ 12 mm bars: yield strength $f_y = 458.67 \text{ N/mm}^2$, ultimate strength $f_u = 570.33 \text{ N/mm}^2$, elastic modulus $E_1 = 206000 \text{ N/mm}^2$ and post-yield hardening ratio $E_2 / E_1 = 0.0032$
- for φ 20 mm bars: yield strength $f_y = 376.67 \text{ N/mm}^2$, ultimate strength $f_u = 567.33 \text{ N/mm}^2$, elastic modulus $E_1 = 206000 \text{ N/mm}^2$ and post-yield hardening ratio $E_2 / E_1 = 0.0056$

The ELSA laboratory features a reaction wall that coupled with a strong floor allows mono-direction pseudo-dynamic tests to be readily carried out (for information on this testing technique readers may refer, for instance, to the overview found in

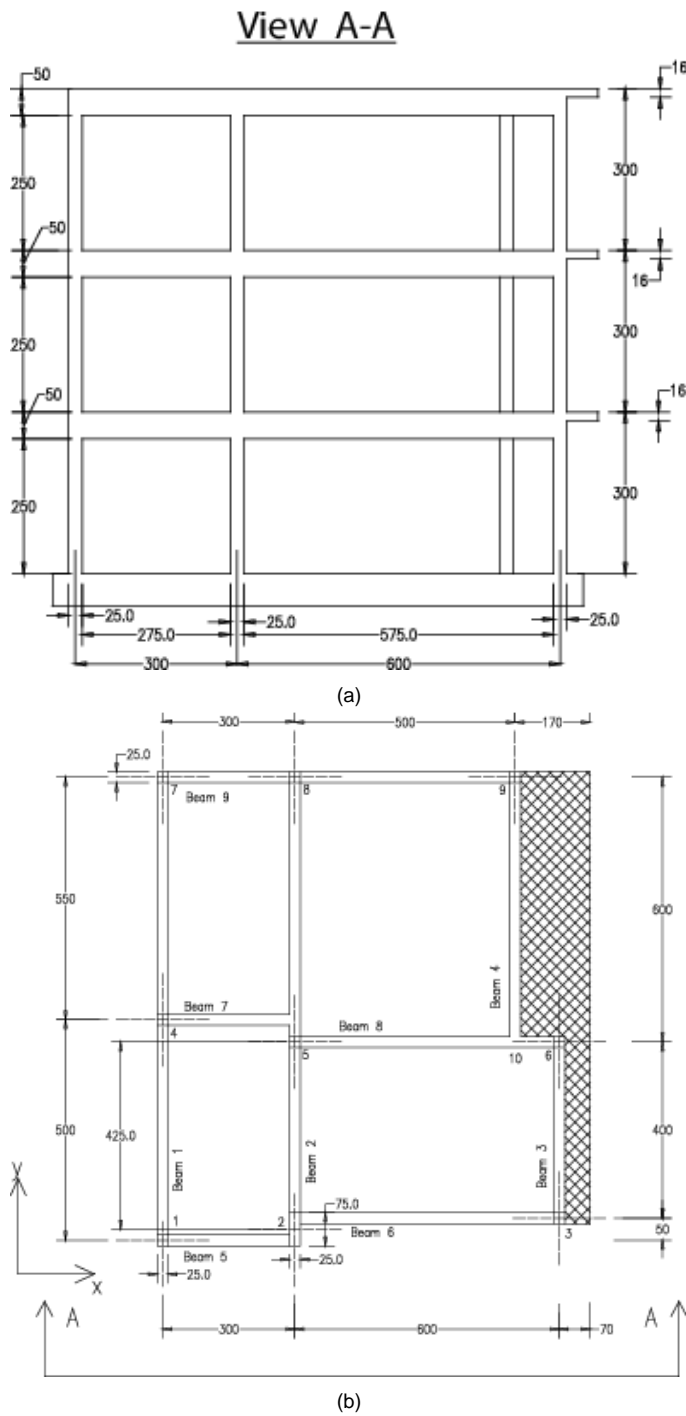


Fig. 1. (a) Side (x-transversal direction) and (b) typical floor views of the real building (geometrical dimension in cm; Fardis [23])

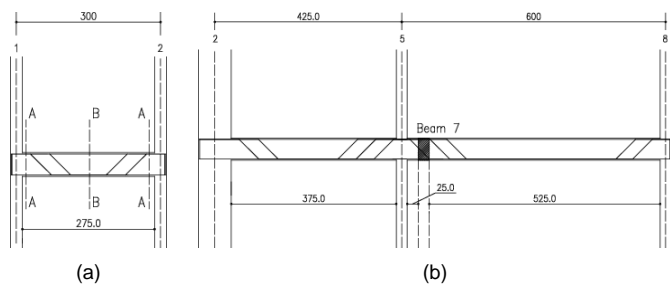


Fig. 2. Geometrical and reinforcement characteristics of (a) beam 5 and (b) beam 2 as defined in Fig. 1

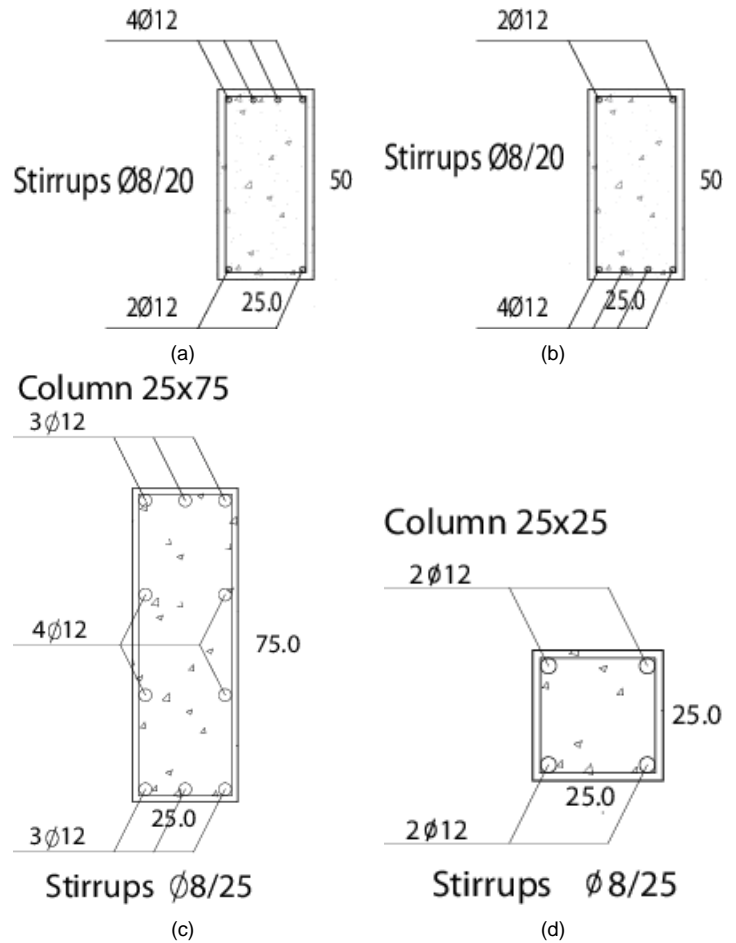


Fig. 3. Details of (a) edge sections of beam 5, (b) mid-span section of beam 5, (c) column 2 cross-section and (d) cross-sections of all other columns (section has been selected with reference to Fig. 2)

Pinho and Elnashai [27] or Sullivan et al. [28]). For the testing of this torsion-sensitive structure, however, it was envisaged that bi-directional loading should be introduced, the reason for which an additional perpendicular reaction braced buttress was constructed and used to cater for bi-directional pseudo-dynamic testing of the building (Mola and Negro [29]; Molina et. al. [30]). The testing campaign consisted of the following four stages:

- 1 preliminary impulse-triggered low-amplitude testing, during which the initial dynamic properties of the structure were obtained (this phase served also the purpose of checking the correct functioning of the complete testing apparatuses and instruments);
- 2 the Herceg-Novti bi-directional accelerogram (registered during the Montenegro 1979 earthquake, and shown in Fig. 4) was applied to the structure in three runs of increasing amplitude (0.02 g, 0.15 g and 0.20 g): under the starting level the structure responded elastically, whilst the subsequent two intensities lead to heavy damage;
- 3 the structure was retrofitted with FRP fibres in those locations where damage was particularly evident, and then was tested again;

4 a final selective strengthening was applied to the most damaged members and another testing campaign was conducted on the re-repaired structure, under intensity seismic input levels that eventually lead to a near-collapse response state.

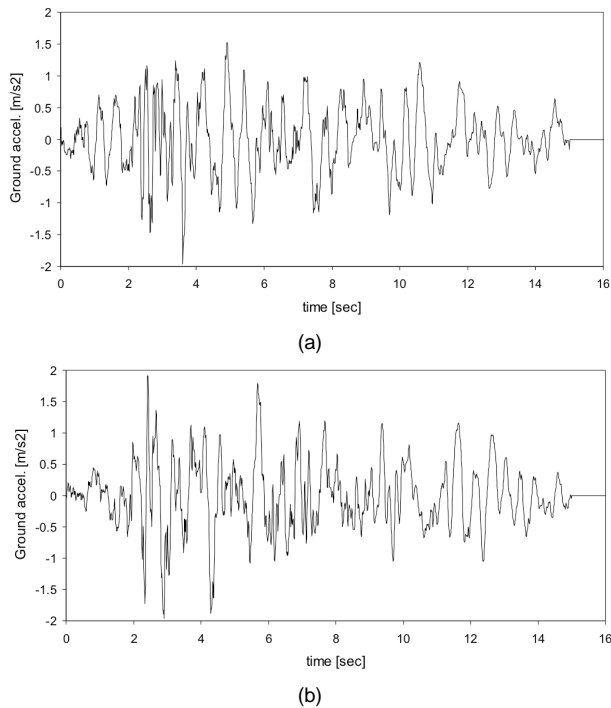


Fig. 4. Herceg-Novı record used in the test of the full scale building: (a) x-direction longitudinal component and (b) y-direction transverse component.

3 Finite element modelling of the prototype structure: verifying the nonlinear analysis tool

As stated above, herein, and in order to verify the accuracy of the numerical tool used in the calibration of the shaking-table testing, an attempt is made to reproduce the results obtained in the aforementioned phases 1 and 2 of the prototype testing, with particular reference to the storey horizontal forces measured by the load cells of the actuators and the floor displacements registered at the numerous transducers located at every single floor slab. Other researchers (e.g. Jeong and Elnashai [26]; Franchin et al. [31]; Fajfar et al. [32]) have already used the results of the SPEAR testing campaign to verify different nonlinear analysis computer codes readily available within the earthquake engineering community. However, in this study, all the time history and pushover analyses will be carried out using SeismoStruct (SeismoSoft [33]), a fibre element-based program for seismic analysis of framed structures featuring a graphics user interface that caters for a relative straightforward creation of error-free models, even by inexperienced users. This computer code incorporates both local (beam-column effects) and global (large displacements/rotations effects) sources of geometric nonlinearity as well as the interaction between axial force and transverse deformation of the element. The employed program has been extensively verified through comparison with experimental results (e.g. Pinho [34]; López-Menjívar [35]; Casarotti and Pinho

[36]; Pietra et al. [37]), to model structural frames in seismic analyses of steel structures (Fagà et al [38], Grande and Rasulo [39], Wijesundara et al. [40–42]), RC buildings (Mpampatsikos et al. [12], Sousa et al. [22]), masonry infill panels (Smyrou et al. [43]) and connections (Brunesi et al. [44, 45]). A finite element model of the SPEAR prototype building was thus created (Fig. 5).

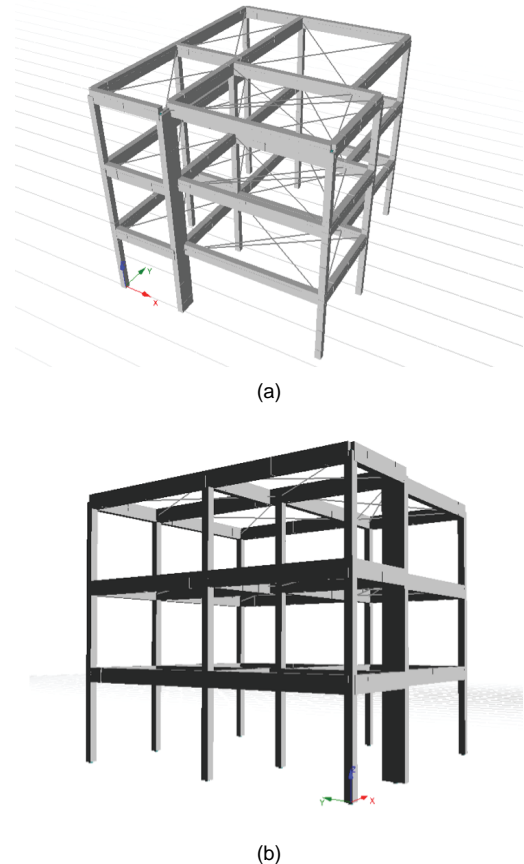


Fig. 5. Overview of the building: rendered views of the finite element model used to reproduce the full scale test

The cross-section of the elements was subdivided into layers of steel and concrete, with the concrete layers following the nonlinear constant confinement model proposed by Mander et al. [46] together with the cyclic relations proposed by Martínez-Rueda and Elnashai [47], whilst the reinforcing steel layers use a very simple and efficient uniaxial bilinear stress-strain model with kinematic strain hardening. As previously described, all columns feature a squared $25 \times 25 \text{ cm}^2$ cross-section, with the exception of column 2 that is instead $25 \times 75 \text{ cm}^2$ (see Fig. 1b) and which called for the modelling depicted in Fig. 6. Inertia mass and vertical loads applied to the model, distributed along columns and beams, represented the (i) self-weight of the frame, (ii) a permanent load of 0.5 kN/m^2 and (iii) a variable load of 2 kN/m^2 .

From the onset it was clear that it would be important to somehow model the horizontal diaphragm effect provided by the slabs of the building, hence an equivalent horizontal truss system was devised and introduced. The slab of the SPEAR specimen was

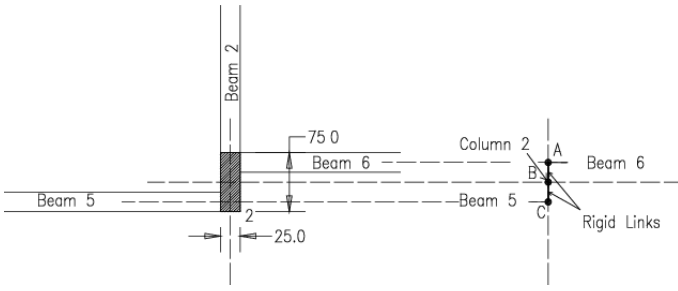


Fig. 6. Modelling of column 2 and its connection to the beams: two rigid link used to put the beams in their geometrical real position in order to account for eccentricity

rigid enough, in order to warrant a correct distribution of inertia forces throughout the structure and also allow an appropriate control of the pseudo-dynamic test. The cross-section dimensions of these fictitious slab braces were computed by equating the in-plane stiffness of the slab to the axial stiffness of the truss element:

$$K_{\text{slab}} = \frac{1}{\frac{(L')^3}{12E_c J} + \frac{L'}{A_s G_c}} = K_{\text{truss}} = \frac{E_{\text{truss}} A_{\text{truss}}}{L_{\text{truss}}} \quad (1)$$

where L' is the main dimension of the slab, J is the in-plane moment of inertia of the transverse section of the slab, E_c is the elastic modulus of the concrete, G_c is computed as $G_c = E_c / (2(1 + \nu))$, A_s is the in-plane shear area, E_{truss} and L_{truss} are respectively the elastic modulus and the length of the truss element.

Firstly, the truss configuration shown in Fig. 7(a), a classical arrangement in which the truss elements converge into the four corners of the slab panels, was attempted, however, the presence of a “free node” between beams 4 and 8 lead to unrealistic in-plane deformations. As a second trial, two extra braces, shown in Fig. 7(b), were introduced to restrain the aforementioned “free node”, leading to an improved modelling of the diaphragm action of the slab. Nonetheless, it was still noted that local spurious deformations were taking place in the intersections between beam 2 and beams 6 and 7. Hence, two further possible configurations (Figs. 7c and 7d), where the truss elements are connected to the barycentre nodes of the columns near the aforementioned beam intersections, were employed.

In Fig. 8, a comparison is made between the x-direction displacement response recorded in node 8 (see Fig. 1b) during the experiment (for the 0.02 g input motion) and the numerical predictions obtained considering the initial (Fig. 7a) and final (Fig. 7d) slab-modelling configurations described above. It is possible to observe that the employment of the horizontal truss arrangement depicted in Fig. 7(d) has lead to a considerable improvement, with respect to the initial configuration, in the obtained response predictions.

Finally, it is perhaps worth noting that alternative slab modelling strategies, such the one proposed by Brunesi et al. in [48], consisting of the use of membrane/shell/solid elements avoid of locking phenomena and spurious energy mode (Nascimbene

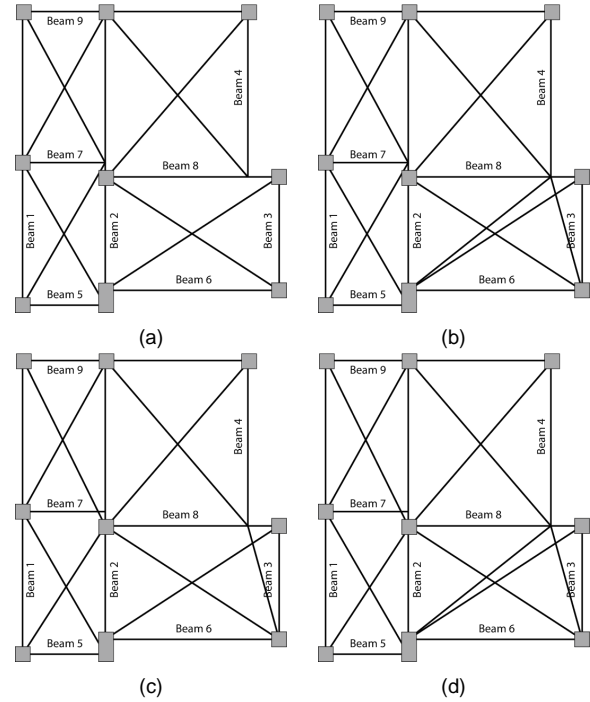


Fig. 7. Equivalent slab modelling configurations using truss element to consider axial flexibility of the floor

[49,50], DellaCroce et al. [51], Nascimbene and Venini [52]) or nodal constrains (Lanese [53]), were seen to lead to essentially identical results with respect to those shown above, obtained using instead an equivalent horizontal truss system. The latter slab modelling scheme, slighter faster and numerically more stable than the former alternatives, was thus adopted for the remaining stages of the study.

4 Comparison between numerical predictions and experimental response: prototype structure

As mentioned above, before each test run, low amplitude vibration was introduced in the building, with a view to allow the identification of the modal properties of the structure, estimated by means of a real-time algorithm developed by Molina et al. [54]. In Table 1, the experimental periods of vibration recorded before the very first test are compared with their corresponding numerical counterparts. As observed, the numerical model is slightly stiffer than the test specimen, as was expected given that the latter had suffered some light damage (i.e. cracking) during the transportation from the outside, where it was built, into the inside of the laboratory, where it was tested (e.g. see Jeong and Elnashai [26] or Fajfar et al. [32]).

Tab. 1. Periods of vibration of prototype structure

	Experimental	Analytical	Difference
T_1	0.85	0.80	5.9%
T_2	0.78	0.72	7.7%

A comparison between the numerical and experimental maxima envelopes for floor displacement (Fig. 9a) and interstorey

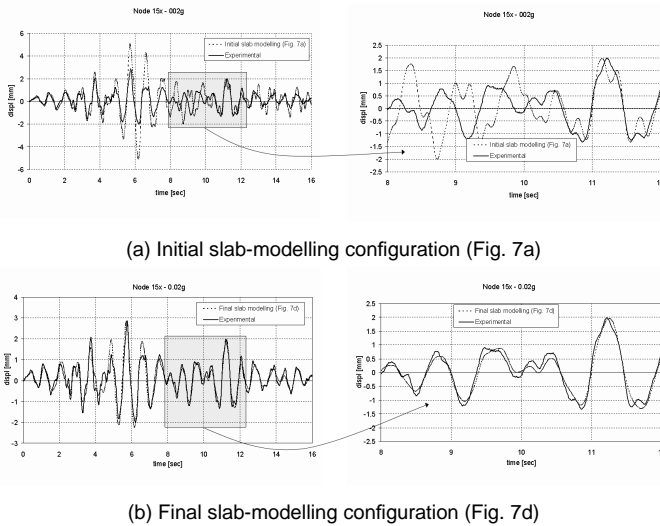


Fig. 8. Experimental-numerical comparison between initial (a) and final (b) slab-modelling configurations

drift (Fig. 9b) profiles is carried out herein. The agreement between is very good for 0.02g (error not greater than 2%) and 0.15g (error less than 7%) intensity levels. On the other hand, a non-negligible underestimation of the displacement and interstorey drift values for the 0.20g accelerogram is visible, this being caused by the fact that, as reported in Jeong and Elnashai [26], the response/deformation mode of the column under these intensity levels was dominated by bar slippage at the beam-column joints (it is recalled that smooth bars were employed in the construction of the test model), something that had not been incorporated in the assembled numerical model.

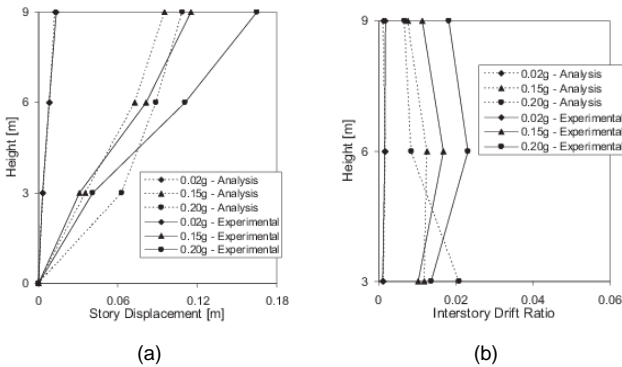


Fig. 9. Numerical and experimental (a) displacement and (b) interstorey drift profile envelopes

In addition to envelope values, also the numerical and experimental displacement response histories at the top/roof level were compared. Whilst the full set of results and comparisons may be found in the work of Lanese [53], herein, and for the sake of brevity, only the displacement histories of node 3 in x-direction and node 10 in y-direction (see Fig. 1b) are shown, in Fig. 10, below. It is observed that the numerical predictions match relatively well the experimental recordings, even if displacement transducers were actually not placed exactly at the

columns/nodes barycentre.

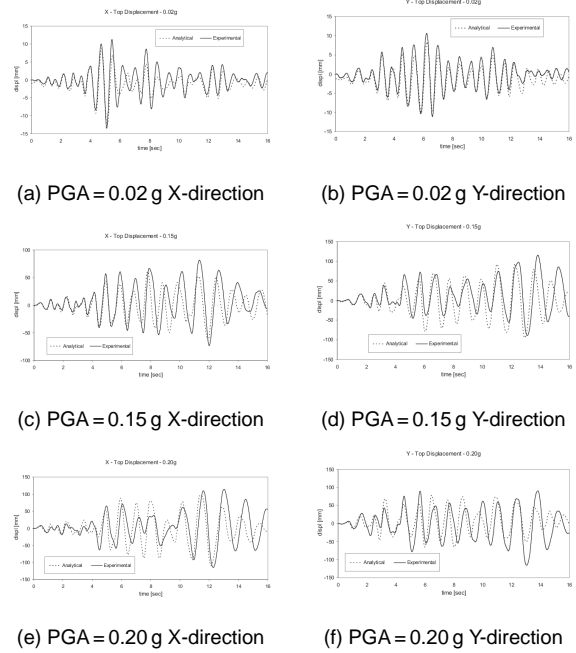


Fig. 10. Experimental and numerical comparison in terms of displacements in X and Y direction corresponding to three level of PGA

A fourth comparison regards the shear forces mobilised by the structure. As in the previous case, an approximation in the comparison is unavoidable because, at each floor level, experimental forces come only from the 4 load cells placed on the heads of the actuators, whilst numerical forces are computed at each column. The two experimental forces for each floor were added and the comparison with the sum of all the numerical shear forces in the same direction was conducted. The agreement between the experimental and numerical values is always good, as shown in Fig. 11.

5 Finite element modelling of the half-scale structure: shaking-table testing of the scaled specimen

For practical reasons, bound to the maximum shaking-table dimensions ($5.6 \times 7.0 \text{ m}^2$) and payload (140 ton), a real scale model was not feasible, hence a geometric scale factor $\lambda = 2$ was considered instead. This implies not only a 50% reduction of the geometrical dimensions of the test specimen, but also that a time reduction factor of $\lambda^{-1/2}$ (i.e. 0.707) and a mass scaling factor of λ^{-2} (i.e. 0.25) must be introduced in order to respect scaling similarity laws (e.g. Sullivan et al. [28]). In this way, it is ensured that response acceleration values and material stresses in the scaled model are identical to those that would have been measured on the prototype. Having validated above the numerical tool through comparisons between the analytical predictions and experimental results of the prototype, a finite element model of the scaled specimen is now created with a view to obtain a realistic prediction of its expected shaking table response, and in this way ensuring that it respects the limits of the shaking table, especially in terms of mobilised total base shear, which

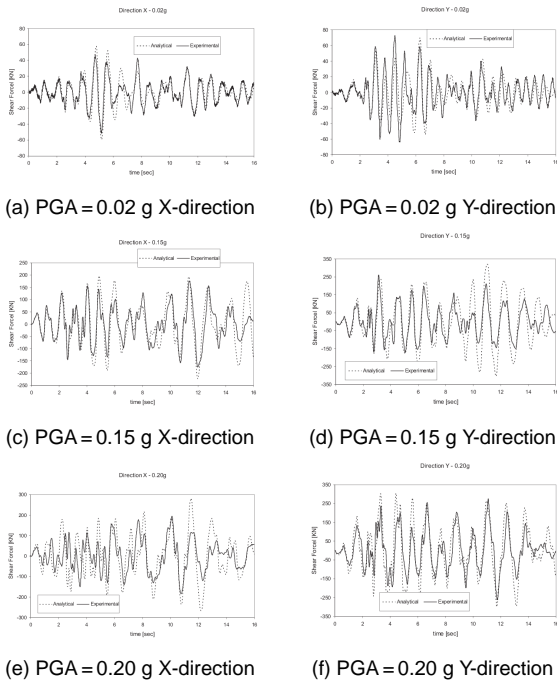


Fig. 11. Experimental and numerical comparison in terms of base shear force

cannot exceed the capacity of the shaking table actuator, equal to 1700 kN (see Calvi et al. [55] for further details on Eucentre’s shaking table).

As a first check on the accuracy of the reduced-scale model, the modal characteristics of the latter are compared in Table 2 with those its prototype counterpart, where it is observed that a relatively good agreement is obtained.

Tab. 2. Periods of vibration of prototype and scaled model

	Prototype (numerical results)	Scaled model (numerical results $\times \sqrt{2}$)	Difference
T_1	0.804	0.826	2.7%
T_2	0.720	0.741	2.9%

Since the dynamic testing of the scaled model will be carried out in one direction only, the corresponding nonlinear time-history analysis are also undertaken in mono-direction fashion (in direction y, according to the global axis convention adopted in Fig. 1, above). Fig. 12 shows the comparison between the base shear forces computed for the prototype and for the scaled specimen, when subjected to an accelerogram with a peak ground acceleration of 0.2 g (it is noted that for the scaled model results, time quantities have been multiplied by a factor $\lambda^{1/2}$ whilst the shears were increased by a factor λ^2).

It is observed that whilst the response of the two structures is quite similar in terms of frequency content, the scaled model tends to lead to lower values of total base shear in the initial part of the response (first 8 seconds), and to higher values of response in the final part of the response history. This change of response trend has been related to issues of damage accumulation in scaled models during transportation (Fig. 14). In

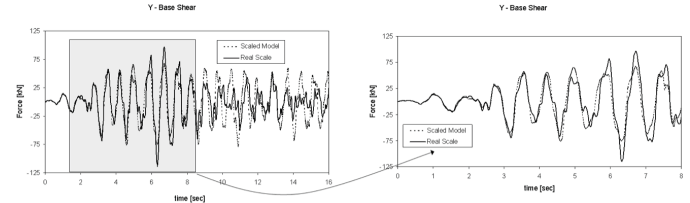


Fig. 12. Comparison between base shear forces in the full and reduced numerical models.

any case, and for what the planning of shaking-table test is concerned, it is reassuring to observe that the mobilised maximum shear forces (around 115 kN, which corresponds to the maximum capacity of the models, as concluded from the capacity curves of Fig. 13) are very much below the aforementioned capacity of the table.

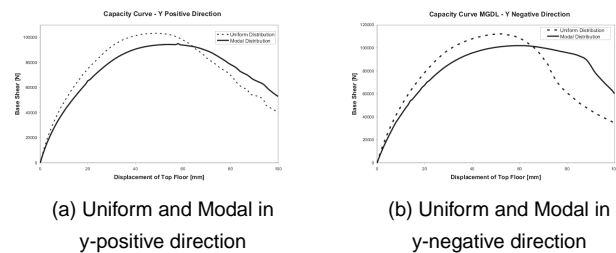


Fig. 13. Pushover curves for the scaled model using two different pushover force distributions



Fig. 14. Scaled specimen (a) during and (b) after construction

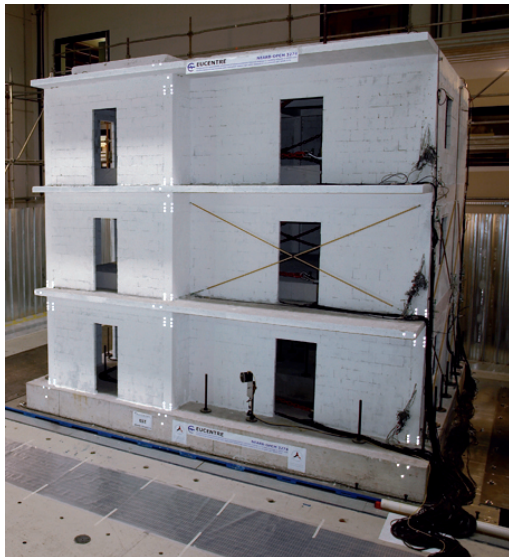
For the sake of completeness, a comparison of response displacements and accelerations between the prototype and scaled models is also shown here (Table 3), even if these results are of reduced importance for what concerns the capacity of the table. It is again observed that the maximum response values of the two structures are similar, attesting once more the adequacy of the scaling and modelling carried out.

It is noted that the final version of the half-scale real structure has been endowed with light infill panel as reported in Fig. 15 and experimentally described by Pavese et al [56].

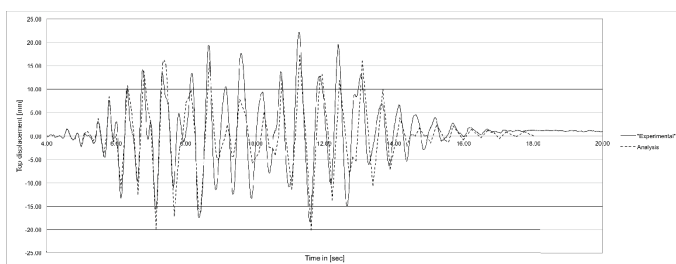
Different kind of infill panels are widely used as partitions, internally and externally to the buildings, but usually they are treated as non-structural elements and are not included in the process of analysis, verification and design. The strong interaction between the infill and the structural frame highly influences the behaviour of the infilled frame by consistently altering globally and locally the load-resisting mechanisms [57, 58].

Tab. 3. Comparison between the prototype and the scaled numerical models

	Displacement (PGA = 0.20 g)		Acceleration (PGA = 0.20 g)	
	Prototype [mm]	half-scaled [mm]	Prototype [m/s ²]	half-scaled [m/s ²]
Y-dir.	± 111	± 54	± 4	± 3.9
X-dir.	± 61	± 30	± 3.6	± 3.3

**Fig. 15.** Scaled specimen with infill panels

A validated model in order to represent the overall response of the infill masonry-frame system as well as the interaction between the infill masonry and the reinforced surrounding frame has been used and based on the research done in the past by Klingner and Bertero [59], Panagiotakos and Fardis [60] and Crisafulli [61]. The advanced nonlinear cyclic model for masonry panels proposed by Crisafulli [61] offers the possibility to model the material with different levels of accuracy taking into account the local phenomena caused by the interaction between infill panel and surrounding frame using an equivalent strut approach. The comparison between experimental and analytical results is shown in Fig. 16.

**Fig. 16.** Experimental and analytical results: a comparison

6 Closing Remarks

In this manuscript, the analytical work carried out in support of an envisaged shaking-table testing campaign was described. The numerical tool that was to be employed in the prediction of the shaking-table response of the specimen was first verified against experimental data from earlier tests on the prototype

structure. The validated FE code was then employed to check if the scaled model was responding as envisaged (i.e. to verify if the geometric/time/mass scaling had been appropriately carried out) and also if the required base shear input was compatible with the table characteristics. Once this preliminary modelling work was completed, the final version of the half-scale infilled frame has been tested and comparison with the numerical model has been carried out.

Acknowledgement

The authors would like to thank the ELSA staff, with particular reference to Dr. Francesco Marazzi, for making the SPEAR project experimental data readily available for this study. Finally, the authors would also like to acknowledge and thank the assistance of Dr. Lorenza Petrini and Dr. Igor Lanese in the modelling of the SPEAR building and of Prof. Alberto Pavese as the coordinator of all experimental activities at the EUCENTRE Laboratory.

References

- 1 **Belleri A, Brunesi E, Nascimbene R, Pagani M, Riva P**, *Seismic performance of precast industrial facilities following major earthquakes in the Italian territory*, Journal of Performance of Constructed Facilities, **29**(5), (2015), 1–10, DOI 10.1061/(ASCE)CF.1943-5509.0000617.
- 2 **Adalier K, Aydingun O**, *Structural engineering aspects of the June 27, 1998 Adana-Ceyhan (Turkey) earthquake*, Engineering Structures, **23**(4), (2001), 343–355, DOI 10.1016/S0141-0296(00)00046-8.
- 3 **Saatcioglu M, Mitchell D, Tinawi R, Gadner NJ, Gillies G, Ghobarah A, Anderson DL, Lau D, Kocaeli (Turkey) earthquake-damage to structures**, Canadian Journal of Civil Engineering, **28**(8), (2001), 715–773.
- 4 **Sezen H, Whittaker AS**, *Seismic performance of industrial facilities affected by the 1999 Turkey earthquake*, Journal of Performance of Constructed Facilities, **20**(1), (2006), 28–36, DOI 10.1061/(ASCE)0887-3828(2006)20:1(28).
- 5 **Toniolo G, Colombo A**, *Precast concrete structures: the lessons learned from the L'Aquila earthquake*, Structural Concrete, **13**, (2012), 73–83, DOI 10.1002/suco.201100052.
- 6 **Brunesi E, Nascimbene R, Bolognini D, Bellotti D**, *Experimental investigation of the cyclic response of reinforced precast concrete framed structures*, PCI Journal, **60**(2), (2015), 57–79.
- 7 **Augenti N, Parisi F**, *Learning from construction failures due to the 2009 L'Aquila, Italy, earthquake*, Journal of Performance of Constructed Facilities, **24**(6), (2010), 536–555, DOI 10.1061/(ASCE)CF.1943-5509.0000122.
- 8 **Ghosh SK, Cleland N**, *Observations from the February 27, 2010, earthquake in Chile*, PCI Journal, **57**(1), (2012), 52–75.
- 9 **Lauciani V, Faenza L, Michelini A**, *ShakeMaps during the Emilia sequence*, Annals of Geophysics, **55**(4), (2012), 631–637, DOI 10.4401/ag-6160.
- 10 **Belleri A, Torquati M, Riva P, Nascimbene R**, *Vulnerability assessment and retrofit solutions of precast industrial structures*, Earthquakes and Structures An International Journal, **8**(3), (2015), 801–820, DOI 10.12989/eas.2015.8.3.801.
- 11 **Bellotti D, Bolognini D, Nascimbene R**, *Response of traditional RC precast structures under cyclic loading*, Environmental Semeiotics, **2**(2), (2009), 63–79.
- 12 **Mpampatsikos V, Nascimbene R, Petrini L**, *A critical review of the r.c. frame existing building assessment procedure according to EUROCODE 8*

- and Italian Seismic Code, *Journal of Earthquake Engineering*, **12**, (2008), 52–82, DOI 10.1080/13632460801925020.
- 13 **Caprili S, Nardini L, Salvatore W**, *Evaluation of seismic vulnerability of a complex RC existing building by linear and nonlinear modeling approaches*, *Bulletin of Earthquake Engineering*, **10**, (2012), 913–954, DOI 10.1007/s10518-011-9329-4.
 - 14 **Calvi GM, Pinho R, Magenes G, Bommer JJ, Restrepo-Vélez LF, Crowley H**, *Development of seismic vulnerability assessment methodologies over the past 30 years*, *ISET Journal of Earthquake Technology*, **43**(3), (2006), 75–104.
 - 15 **Whitmann RV, Reed JV, Hong ST**, *Earthquake damage probability matrices*, 5th World Conference on Earthquake Engineering, In: Rome, Italy, 1973-06-25, pp. 2531–2540.
 - 16 **Faccioli E, Pessina V, Calvi GM, Borzi B**, *A study on damage scenarios for residential buildings in Catania city*, *Journal of Seismology*, **3**, (1999), 327–343, DOI 10.1023/A:1009856129016.
 - 17 **Sabetta F, Goretti A, Lucantoni A**, *Empirical fragility curves from damage surveys and estimated strong ground motion*, 11th European Conference on Earthquake Engineering, In: Paris, France, 1998-09-06, pp. 1–11.
 - 18 **Casotto C, Silva V, Crowley H, Nascimbene R, Pinho R**, *Seismic Fragility of Italian RC Precast Industrial Structures*, *Engineering Structures*, **94**, (2015), 122–136, DOI 10.1016/j.engstruct.2015.02.034.
 - 19 **Singhal A, Kiremidjian AS**, *Method for probabilistic evaluation of seismic structural damage*, *Journal of Structural Engineering ASCE*, **122**(12), (1996), 1459–1467, DOI 10.1061/(ASCE)0733-9445.
 - 20 **Cosenza E, Manfredi G, Verderame GM**, *A new strategy for the seismic assessment of existing RC buildings*, *Annals of Geophysics*, **45**(6), (2002), 817–831, DOI 10.4401/ag-3545.
 - 21 **Masi A**, *Seismic vulnerability assessment of gravity load designed R/C frames*, *Bulletin of Earthquake Engineering*, **1**(3), (2003), 371–395, DOI 10.1023/B:BEEE.0000021426.31223.60.
 - 22 **Sousa R, Bianchi F, Pinho R, Nascimbene R, Kazantzidou D**, *Modelling issues on seismic assessment of irregular RC structures*, *COMPADYN 2011 3rd International Conference on Computational Methods in Structural Dynamics and Earthquake Engineering*, In: Corfu, Greece, 2011-05-25, pp. 1–16.
 - 23 **Fardis MN**, *Design of an Irregular Building for the SPEAR Project - Description of the 3-Storey Structure*, University of Patras, 2002.
 - 24 **Coelho E, Campos Costa A, Candeias P, Silva MJF, Mendes L**, *Shake table tests of a 3-storey irregular RC structure design for gravity loads*, *International Workshop SPEAR*, In: Ispra, Italy, 2005-04-04, pp. 123–138.
 - 25 **Fardis MN, Negro P**, *SPEAR - Seismic performance assessment and rehabilitation of existing buildings*, *Proceedings of the International Workshop on the SPEAR Project*, In: Ispra, Italy, 2005-04-04, pp. 1–304.
 - 26 **Jeong SH, Elnashai AS**, *Analytical assessment of the seismic performance of an irregular RC frame for full scale 3D pseudo-dynamic testing, Part I: analytical model verification*, *Journal of Earthquake Engineering*, **9**(1), (2005), 95–128.
 - 27 **Pinho R, Elnashai AS**, *Dynamic collapse testing of a full-scale four storey RC frame*, *ISET Journal of Earthquake Engineering*, **37**(4), (2000), 143–164.
 - 28 **Sullivan TJ, Pinho R, Pavese A**, *An introduction to structural testing techniques in earthquake engineering*, IUSS Press, 2004.
 - 29 **Mola E, Negro P**, *Full scale PsD testing of the torsionally unbalanced SPEAR structure in the as-built and retrofitted configurations*, *Proceedings of the International Workshop on the SPEAR Project*, In: Ispra, Italy, 2005-04-04, pp. 139–154.
 - 30 **Molina FJ, Buchet P, Magonette GE, Hubert O, Negro P**, *Full-scale bidirectional PsD testing of the torsionally unbalanced SPEAR structure: method, algorithm and experimental set-up*, *Proceedings of the International Workshop on the SPEAR Project*, In: Ispra, Italy, 2005-04-04, pp. 155–188.
 - 31 **Franchin P, Lupoi A, Pinto PE, Schotanus MI**, *Seismic fragility analysis of RC structures: use of response surface for a realistic application*, *Proceedings of the International Workshop on the SPEAR Project*, In: Ispra, Italy, 2005-04-04, pp. 99–110.
 - 32 **Fajfar P, Dolsek M, Marusic D, Stratan A**, *Pre- and post-test mathematical modelling of a plan-asymmetric reinforced concrete frame building*, *Earthquake Engineering and Structural Dynamics*, **35**, (2006), 1359–1379, DOI 10.1002/eqe.583.
 - 33 **SeismoStruct - A computer programme for static and dynamic nonlinear analysis of frames structures**, SeismoSoft; Italy, 2015.
 - 34 **Pinho R**, *Shaking table testing of RC walls*, *ISET Journal of Earthquake Engineering*, **37**(4), (2000), 119–142.
 - 35 **Lopez-Menjivar MA**, *Verification of a displacement-based Adaptive Pushover method for assessment of 2-D Reinforced Concrete Buildings*, PhD thesis, European School for Advances Studies in Reduction of Seismic Risk (ROSE School), 2004.
 - 36 **Casarotti C, Pinho R**, *Seismic response of continuous span bridges through fibre-based finite element analysis*, *Journal of Earthquake Engineering and Engineering Vibration*, **5**(1), (2006), 119–131, DOI 10.1007/s11803-006-0631-0.
 - 37 **Pietra D, Pinho R, Antoniou S**, *Verification of displacement-based adaptive pushover for seismic assessment of high-rise steel buildings*, *First European Conference on Earthquake Engineering and Seismology*, In: Geneva, Switzerland, 2006-09-03, pp. 1–10.
 - 38 **Faga E, Rassati GA, Nascimbene R**, *Seismic design of elevated steel tanks with concentrically braced supporting frames*, *Structures Congress 2012*, In: Chicago, USA, 2012-03-29, pp. 1473–1484.
 - 39 **Grande E, Rasulo A**, *Seismic assessment of concentric X-braced steel frames*, *Engineering Structures*, **49**, (2013), 983–995, DOI 10.1016/j.engstruct.2013.01.002.
 - 40 **Wijesundara KK, Bolognini D, Nascimbene R, Calvi GM**, *Review of design parameters of concentrically braced frames with RHS shape braces*, *Journal of Earthquake Engineering*, **13**, (2009), 109–131, DOI 10.1080/13632460902813331.
 - 41 **Wijesundara KK, Nascimbene R, Sullivan TJ**, *Equivalent viscous damping for steel concentrically braced frame structures*, *Bulletin of Earthquake Engineering*, **9**(5), (2011), 1535–1558, DOI 10.1007/s10518-011-9272-4.
 - 42 **Wijesundara KK, Nascimbene R, Rassati GA**, *Modelling of different bracing configuration in multi-storey concentrically braced frames using a fiber-beam based approach*, *Journal of Constructional Steel Research*, **101**, (2014), 426–436, DOI 10.1016/j.jcsr.2014.06.009.
 - 43 **Smyrou E, Blandon C, Antoniou S, Pinho R, Crisafulli F**, *Implementation and verification of a masonry panel model for nonlinear dynamic analysis of infilled RC frames*, *Bulletin of Earthquake Engineering*, **9**(5), (2011), 1519–1534, DOI 10.1007/s10518-011-9262-6.
 - 44 **Brunesi E, Nascimbene R, Rassati GA**, *Response of partially-restrained bolted beam-to-column connections under cyclic loads*, *Journal of Constructional Steel Research*, **97**, (2014), 24–38, DOI 10.1016/j.jcsr.2014.01.014.
 - 45 **Brunesi E, Nascimbene R, Rassati GA**, *Evaluation of the response of partially restrained bolted beam-to-column connection subjected to cyclic pseudo-static loads*, *Structures Congress 2013*, In: Pittsburgh, USA, 2013-05-02, pp. 2310–2321.
 - 46 **Mander JB, Priestley MJN, Park R**, *Theoretical stress-strain model for confined concrete*, *ASCE Journal of Structural Engineering*, **114**(8), (1988), 1804–1826, DOI 10.1061/(ASCE)0733-9445.
 - 47 **Martinez-Ruend JE, Elnashai AS**, *Confined concrete model under cyclic load*, *Materials and Structures*, **197**(39), (1997), 139–147, DOI 10.1007/BF02486385.
 - 48 **Brunesi E, Bolognini D, Nascimbene R**, *Evaluation of the shear capacity of precast-prestressed hollow core slabs: numerical and experimental comparisons*, *Materials and Structures*, **48**, (2015), 1503–1521, DOI 10.1617/s11527-014-0250-6.

- 49 **Nascimbene R.** *Towards non-standard numerical modeling of thin-shell structures: geometrically linear formulation*, International Journal of Computational Methods in Engineering Science and Mechanics, **15**(2), (2014), 126–141, DOI 10.1080/15502287.2013.874058.
- 50 **Nascimbene R.** *An arbitrary cross section, locking free shear-flexible curved beam finite element*, International Journal of Computational Methods in Engineering Science and Mechanics, **14**(2), (2013), 90–103, DOI 10.1080/15502287.2012.698706.
- 51 **Dellacroce L, Venini P, Nascimbene R.** *Numerical simulation of an elastoplastic plate via mixed finite elements*, Journal of Engineering Mathematics, **46**, (2003), 69–86, DOI 10.1023/A:1022836202029.
- 52 **Nascimbene R, Venini P.** *A new locking-free equilibrium mixed element for plane elasticity with continuous displacement interpolation*, Computer Methods in Applied Mechanics and Engineering, **191**, (2002), 1843–1860, DOI 10.1016/S0045-7825(01)00356-5.
- 53 **Lanese I.** *Valutazione numerico-sperimentale del comportamento sismico di un edificio esistente progettato per soli carichi verticali*, Final Year Graduation Thesis, Department of Structural Mechanics, University of Pavia, 2006.
- 54 **Molina FJ, Pegon P, Verzeletti G.** *Time-domain identification from seismic pseudodynamic test results on civil engineering specimens*, Proceedings of the Second International Conference on Identification in Engineering Systems, In:; Kissimmee, Florida, 1999-03-02, pp. 1–10.
- 55 **Calvi G M, Pavese A, Ceresa P, Dacarro F, Lai CG, Beltrami C.** *Design of a Large-scale Dynamic and Pseudo-dynamic Testing Facility*, IUSS Press, 2005.
- 56 **Lanese I, Pavese A, Nascimbene R.** *Seismic vulnerability assessment of an infilled reinforced concrete frame structure designed for gravity loads*, 2015. accepted for publication Journal of Earthquake Engineering.
- 57 **Bruggi M.** *Finite element analysis of no-tension structures as a topology optimization problem*, Structural and Multidisciplinary Optimization, **50**(6), (2014), 957–973, DOI 10.1007/s00158-014-1093-z.
- 58 **Bruggi M, Talierno A.** *Analysis of no-tension structures under monotonic loading through an energy-based method*, Computers and Structures, **159**, (2015), 14–25, DOI 10.1016/j.compstruc.2015.07.002.
- 59 **Klingner RE, Bertero VV.** *Earthquake Resistance of Infilled Frames*, ASCE Journal of the Structural Division, **104**, (1978), 973–989.
- 60 **Panagiotakos TB, Fardis MN.** *Proposed Nonlinear Strut Models for In-fill Panels 1st Year Progress Report of HCM-PREC8 Project*, University of Patras, 1994.
- 61 **Crisafulli F J.** *Seismic Behaviour of Reinforced Concrete Structures with Masonry Infills*, PhD Thesis, University of Canterbury, 1997.